Journal of Applied Polymer Science

Second modification of a polyamide membrane surface

Ahmad Akbari, Saeedeh Mohtasham Khani, Seyed Majid Mojallali Rostami
Institute of Nanoscience and Nanotechnology, University of Kashan, Kashan, Islamic Republic of Iran
Correspondence to: A. Akbari (E-mail: akbari@kashanu.ac.ir)

ABSTRACT: The aim of this study was to develop the water flux and antifouling properties of a polyamide (PA) nanofiltration membrane. A nascent PA membrane was prepared with an interfacial polymerization technique and modified with 2,5-diaminobenzene sulfonic acid (2,5-DABSA) as a second modification. The effects of the 2,5-DABSA monomer concentration and the modification time on the membrane performance were investigated. The chemical structure, morphology, roughness, hydrophilicity, molecular weight cutoff, and antifouling properties of the membranes were characterized by Fourier transform infrared spectroscopy, scanning electron microscopy, atomic force spectroscopy, contact angle measurement, poly(ethylene glycol) tracers, and cetyl trimethyl ammonium bromide filtration, respectively. The PA membrane with optimized performance was shown to have a greater than 44% higher water permeate flux with a change in the salt rejection in the order $RNa_2SO_4 > RCaCl_2 > RNaCl$ to $RNa_2SO_4 > RNaCl > RCaCl_2$. The improvement of the hydrophilicity led to excellent antifouling properties in the new PA membranes and illustrated a promising and simple method for the fabrication of high-performance PA membranes. © 2016 Wiley Periodicals, Inc. J. Appl. Polym. Sci. **2016**, *133*, 43583.

KEYWORDS: membranes; polyamides; synthesis and processing

Received 20 December 2015; accepted 24 February 2016
DOI: 10.1002/app.43583

INTRODUCTION

The polymeric membrane process is a desired technology for water and wastewater treatment because it does not require a phase change to make a separation and has a low energy consumption.[1,2] Nanofiltration membranes exhibit separation performance in the intermediate range between reverse osmosis and ultrafiltration processes; this performance was expanded in the 1980s on the basis of reverse osmosis membranes by Cadotte and coworkers.[3–5] It has received much interest because of many its advantages, including a high permeate flux, high salt rejection, intermediate operating pressure, low primary investment and operating costs, and wide applicability, such as in water softening, dye removal, organic removal, and chemical and biological oxygen demand reduction. It has a variety of uses in pharmaceuticals, semiconductors, paper, and the dairy and food industries.[6–10] Nowadays, the interfacial polymerization technique is considered a general method that is widely used for the fabrication of polyamide (PA) nanofiltration and reverse osmosis membranes.[11] Increasing the water permeate flux of PA nanofiltration membranes reduces the operation pressure and time and leads to a decrease in the energy consumption and a longer life. However, one of the major challenges to the widespread application of PA nanofiltration membranes is surface fouling during the filtration time.[12] In the fouling process, foulants (solute or particles) in feed solutions are deposited onto the PA surface or pores, so the membrane performance is degraded; this results in the decline of the water permeate flux and salt selectivity. Membrane fouling increases the resistance that occurs during filtration by the reversible and irreversible deposition of components in the feed solution on the hydrophobic membrane surface.[13,14] Membrane fouling arises from two origins: (1) the physicochemical properties of the membrane surface, such as the hydrophilicity, roughness, electrostatic charge, and morphology and (2) solute type in water or wastewater, including organic, inorganic, colloidal, and biological agents.[15,16]

Hence, a large number of studies have been carried out to develop antifouling properties and produce high-performance and resistant membranes. Different techniques have been applied to improve the antifouling properties of PA membranes; these include the use of new monomers and additives in the interfacial polymerization reaction, physical methods (surface adsorption and surface coating), chemical methods (hydrophilization, radical grafting, chemical coupling, plasma polymerization and initiated chemical vapor deposition), and preparation of hybrid PA membranes with inorganic particles.[17–22] New monomers with higher polar properties or functional groups can be created by a new PA layer with a smoother surface roughness, higher hydrophilicity, and different surface charge. It is well known that compounds containing sulfonic acid groups are effective monomers for the development of the water permeate flux, antifouling properties, and surface charge of the membrane.[23] Wang *et al.*[24] prepared PA

nanofiltration membranes with two types of novel sulfonated aromatic diamine monomers, 2,5-bis(4-amino-2-trifluoromethylphenoxy)benzene sulfonic acid and 4,4′-bis(4-amino-2-trifluoromethyl phenoxy)biphenyl-4,4′-disulfonic acid. The lower diffusion rates of the two types of sulfonate diamines and the swollen PA active skin layer led to a negative membrane performance. Because the molecular weight growth of the PA was restricted because of the lower diffusion and steric hindrance of the sulfonic acid groups, this resulted in a low density degree and weak active skin layer of PA. Freeman *et al.*[25] synthesized a PA membrane with disulfonated bis[4-(3-aminophenoxy)phenyl]sulfone. The resulting membranes had a lower sodium chloride (NaCl) rejection and reduced chlorine tolerances with a little higher water permeate flux. The use of new monomers affected the interfacial polymerization reaction and PA layer properties, including the PA polymer molecular weight growth, diamine diffusion, kinetics and reaction rate, density of the PA layer, pore size, morphology, roughness, and hydrophilicity. In general, the use of a sulfonated monomer in an interfacial polymerization reaction will result in some positive (higher hydrophilicity or permeate flux) and negative (higher roughness, swelling, and lower rejection) effects. Zhang *et al.*[26] carried out interfacial polymerization with *m*-phenylene diamine, *m*-phenylene diamine-5-sulfonic acid (SMPD), and trimesoyl chloride (TMC). The NaCl rejection of the reverse osmosis membranes decreased, and the water flux increased when the weight ratio of SMPD increased. The linear part of the PA polymer with pendant —COOH increased with enhanced SMPD concentration and led to a smoother membrane surface.

In this article, we report a promising strategy for using sulfonic acid effects and developing hydrophilicity and antifouling properties by the secondary modification of a PA membrane. The PA membrane was prepared with the interfacial polymerization between piperazine (PIP) and triethylamine (TEA) in the aqueous phase and TMC in the organic phase. Then, fresh PA membrane was immersed immediately into 2,5-diaminobenzene sulfonic acid (2,5-DABSA) monomer in an aqueous solution for second modification reaction. The water permeate flux and different salt rejections of the membranes were examined with a crossflow filtration device. Changes in the membrane chemical compositions were studied by Fourier transform infrared (FTIR) spectroscopy. The surface morphology and roughness were determined by scanning electron microscopy (SEM) and atomic force spectroscopy (AFM) analysis, respectively. The hydrophilicity of the membrane surfaces was investigated by the determination of the contact angles of the membrane surfaces. Also, the molecular weight cutoffs (MWCOs) of the PA membrane before and after modification with the 2,5-DABSA monomer was traced through the different molecular weights of poly(ethylene glycol) (PEG). The antifouling properties of the PA nanofiltration membranes were tested with a cetyl trimethyl ammonium bromide (CTAB) aqueous solution (1500 ppm).

EXPERIMENTAL

Materials

Polysulfone (PSf; number-average molecular weight = 17,000 g/mol, molecular weight = 35 kDa) was manufactured by Sigma Aldrich Co. *N,N*-Dimethylformamide (DMF) was used as a PSf solvent. TMC was used as the active monomer in the organic phase. PIP was used as the active monomer in the aqueous phase. 2,5-DABSA was used as the active monomer the for second modification. TEA was used as a proton acceptor. *n*-Hexane, CTAB, NaCl, sodium sulfate (Na_2SO_4), calcium chloride ($CaCl_2$), and PEGs (molecular weights = 1000, 2000, 3000, and 6000 Da) were obtained from Merck Chemicals (Germany) and were used without further purification.

Preparation of the Membrane

Preparation of the PSf Substrate. The PSf asymmetric substrates were prepared by the classical immersion precipitation phase inversion method. A homogeneous PSf casting solution was prepared by the dissolution of PSf (18% w/w) and PEG 6000 Da (8% w/w) in DMF (74% w/w) solvent with stirring at 500 rpm for 24 h at 80 °C. All casting solutions were held under air conditions at room temperature for 2 h to remove the air bubbles. The polymer solutions were cast uniformly onto a glass substrate with a hand-casting knife (gap = 250 μm) and immediately immersed in a coagulating water bath with at a temperature of 25 ± 1 °C. The substrate remained at least overnight until most of the DMF solvent and PEG (as a pore former) were removed, and the PSf substrate frame was completely formed. The PSf substrates were then washed thoroughly with deionized water and stored in water at room temperature until they were tested.

Fabrication of the PA Membrane. The active skin layer of PA was created on the PSf substrate through a conventional interfacial polymerization method. The PSf substrate was soaked in an aqueous phase solution containing 2% w/w PIP and 0.6% w/w TEA for 2 min. The diamine-loaded PSf substrate was drained with a soft rubber roller until the bubbles and excess solution were eliminated from the PSf substrate surface and, finally, no liquid from the diamine solution remained. After the bubbles and excess solution were drained, the PSf substrate was clamped between two Teflon frames. Subsequently, the organic phase solution of 0.1% w/v TMC in *n*-hexane was poured into the frame. After a predetermined interfacial polymerization reaction period (60 s), the organic phase solution was drained off. Then, the prepared PA membranes were washed and stored in deionized water (4 ± 1 °C) before the evaluation studies.

Second Modification of the PA Surface with 2,5-DABSA

For the second modification of the PA membranes, a 2,5-DABSA monomer solutions were used with different concentrations (0.1, 0.5, and 1% w/w) and coagulation times (5, 10, and 15 min). After interfacial polymerization, the prepared PA membranes without washing were immediately immersed into the 2,5-DABSA monomer solution to react with the free acyl chloride groups with new diamines as a second modification. Then, these new PA membranes were washed and stored in deionized water at 4 ± 1 °C for further experiments.

Membrane Performance Test

Experimental experiments were carried out with a batch crossflow system with a membrane module with a 21-cm^2 effective surface area. The water permeate flux (±1.5 L m^{-2} h^{-1}) and salt rejection of NaCl (±1), Na_2SO_4 (±2), and $CaCl_2$ (±2)

were measured with a total concentration of 1000 ppm of salts at 25 ± 1 °C (the feed solution temperature was fixed by a cooling system), a 3-bar pressure, and a 6 L/min flow rate for all of the tests. The water flux (J; L m^{-2} h^{-1}) values of the PA membranes were determined by the direct measurement of the water permeate volume, which was calculated by the following equation:

$$J = V/(At) \quad (1)$$

where V is the volume of permeated water (L), A is the effective membrane surface area (m^2), and t is the filtration time (h). The solute concentration of permeation flux was measured by a conductivity meter and the standard calibration curve of each salt. The membrane rejection was calculated with the following equation to evaluate its desalination performance:

$$\text{Rejection } (\%) = \left[1-\left(C_p/C_f\right)\right] \times 100 \quad (2)$$

where C_p and C_f are the permeate and feed solution concentrations (mg/L), respectively. To minimize water flux and salt concentration measurement error, all of the experiments were carried out three times, and the average value was reported. Also, the water permeate flux and salt rejections were recorded for all of the membrane samples when their performance reached steady state.

Characterization of the Membranes

The chemical properties and structures of the synthesized PA membranes were characterized by FTIR spectroscopy (Nicolet MagnaIR 550) in the region 400–4000 cm^{-1}. The membrane surface morphological properties were determined by SEM (SEM KYKY-EM 3200, China) and AFM (Park Scientific Instrument, CP Auto Probe). We obtained the SEM images by coating the surface membranes with gold before imaging. The surface AFM images were obtained over different areas of every sample. In this analysis, tapping mode of the AFM apparatus was used, and the same tip was applied when we scanned the surfaces of all of the membrane samples. All of membrane samples were prepared in the same way (same temperature, air medium, and scale) to obtain the AFM images. The average roughness (S_a), root mean square of the Z data (S_q), and maximum point height (S_z) were determined over an area of 2 × 2 μm^2.

The hydrophilicity of the PSf substrate and PA membrane surfaces were determined by the measurement of the pure water contact angle with a contact angle goniometer from Drop Shape Analysis (DSA 100 KRUSS GMBH, Hamburg) at room temperature. At least five measurements at different locations were obtained for each membrane, and these were averaged to determine the contact angle values. To measure the membranes contact angles, 4 μL of deionized water was poured onto the surface with a microsyringe. The image of the water and membrane was recorded after 3 s, and the contact angle value was measured.

The MWCO is a membrane pore characteristic that is achieved by neutral organic compounds. Usually, PEG is used to measure the MWCO value because it has a wide range of molecular weights and at least interacts with itself and the membrane surface. A set of reference PEG compounds with different molecular weights (1000, 2000, and 3000) was chosen.[22] Wherever PEG rejection by the membrane reached 90%, the MWCO was measured, and the membrane pore size was calculated from the relationship between the molecular weight of PEG and its Stokes radius as follows[28,29]:

$$r_{hyd} = \left(\frac{3[\eta]MM_{PEG}}{4\pi\varepsilon N}\right)^{\frac{1}{3}} \quad (3)$$

$$[\eta] = 4.9 \times 10^{-8}(MM_{PEG})^{0.672} \quad (4)$$

where $[\eta]$ is the intrinsic viscosity of the solution (m^3/g), MM_{PEG} is the molecular weight of PEG on the border of 90% (g/mol), ξ is the constant proportionality of the PEG polymer molecule between the equivalent sphere and the gyration radius, and N is Avogadro's number (mol^{-1}). The PEG concentrations in the permeate and feed solutions were calculated with $BaCl_2$ and I_2/KI reagents and a UV–visible absorption spectrophotometer at 535 nm.[30] Also, standard calibration curves were drawn for each PEG molecular weight with the Causserand method.

The antifouling properties of the PA nanofiltration membranes were investigated by filtration of a 1500-ppm CTAB feed solution. The flux recovery ratio (FRR), reversible fouling ratio (R_r), irreversible fouling ratio (R_{ir}), and total resistance (R_t) of each membrane were calculated as follows[31,32]:

$$\text{FRR} = (J_{w2}/J_{w1}) \times 100 \quad (5)$$

$$R_r(\%) = \left[\left(J_{w2}-J_p\right)/J_{w1}\right] \times 100 \quad (6)$$

$$R_{ir}(\%) = \left[(J_{w1}-J_{w2})/J_{w1}\right] \times 100 \quad (7)$$

$$R_t = R_r + R_{ir} \quad (8)$$

where J_{w1} is the water permeate flux (L m^{-2} h^{-1}) calculated with eq. (1) and J_p is the permeate flux of the CTAB feed solution during 4 h. Next, the membrane was washed with deionized water for 10 min, and the permeate water flux of the cleaned membranes was measured again as illustrated by J_{w2}.

RESULTS AND DISCUSSION

Feasibility of the PA Membrane Modification

In this study, a PIP aliphatic monomer as a reactant, TEA as an acid acceptor in the aqueous phase, and TMC as an aromatic monomer reactant in the organic phase were used for the interfacial polymerization reaction onto the PSf substrate surface. Since, the PA active skin layer determined the final specifications of the composite membrane, including the water permeate flux, selectivity, morphology, roughness, hydrophilicity, and antifouling properties, to improve the membrane performance, a second modification was necessary. Therefore, the feasibility of a second modification with 2,5-DABSA monomer onto the PA layer was examined. The investigation of the interfacial polymerization mechanism showed that diamines from aqueous phase diffusion passed among the formed PA layer and, in the organic phase, reacted with the TMC monomer.[30,35] When the reaction time was increased, the thickness of the PA layer increased, and the diamine diffusion rates into the organic phase decreased. This phenomenon led to more reminders of free acyl chloride groups on the nascent PA layer. As shown in the schematic in Figure 1, immediately after the interfacial polymerization reaction, the membrane surface contained a large number of free acyl chloride groups; these could be used for the

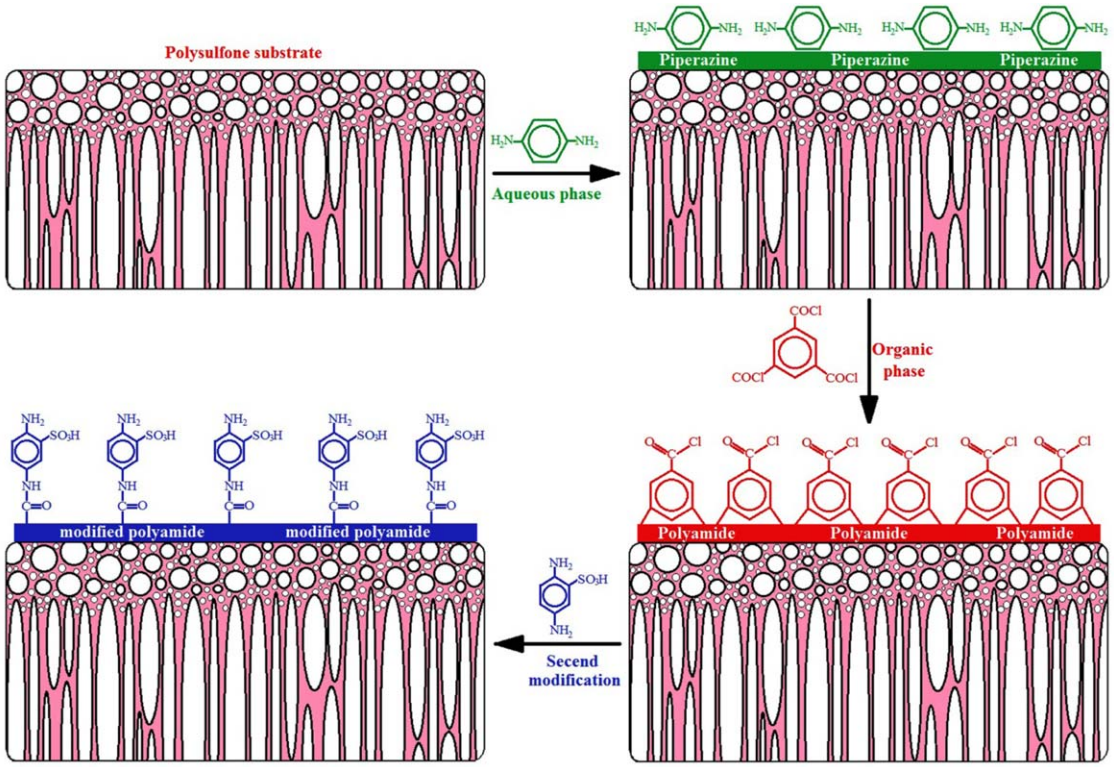

Figure 1. Scheme of interfacial polymerization and second modification. [Color figure can be viewed in the online issue, which is available at wileyonlinelibrary.com.]

second modification of the PA membrane surface. In this step, the 2,5-DABSA monomer with two amine groups was used for the reaction with acyl chloride groups and one sulfonic acid group to increase the properties and performance of PA nanofiltration membranes. The formation of the PA layer was done by a classical interfacial polymerization technique without any changes in the reaction conditions, PA thickness, length of PA polymer chain, morphology, or roughness. Increasing the water permeate flux, hydrophilicity, and antifouling properties were goals of this study.

Optimization of the 2,5-DABSA Concentration

The PA membranes were prepared by interfacial polymerization between PIP (2% w/w) and TEA (0.6% w/w) in the aqueous phase and TMC (0.1% w/v) in the organic phase at 60 s. The reached PA membranes showed acceptable performance with a 14.3 L m^{-2} h^{-1} water permeate flux and 25.5, 87.1, and 55.2% salt rejections of NaCl, Na_2SO_4 and $CaCl_2$, respectively. The nascent PA layer contained a large number of free acyl chloride groups; as a result, it was possible to modify the PA layer with 2,5-DABSA monomer. Different concentrations of 2,5-DABSA monomer (0.1, 0.5, and 1% w/w) were used for the second modification of the PA membrane surface. Also, the modification time of the PA membrane for all of the samples in this step was 5 min. The PA membranes were thoroughly immersed in the 2,5-DABSA monomer solution and shaken several times until all of the bubbles were removed. The effects of the 2,5-DABSA monomer concentrations on the water permeability flux are shown in Figure 2. As shown, the 2,5-DABSA monomer concentration extensively affected the water permeability when compared with the primary PA membranes. When the 2,5-DABSA monomer concentration was increased, the water permeate flux was enhanced from 14.3 L m^{-2} h^{-1} in the PA membrane without the second modification to 18.9 L m^{-2} h^{-1} at a 0.5% w/w 2,5-DABSA monomer concentration; this was a 32% enhancement over the unmodified PA membrane. The higher water permeate flux was attributed to the higher polarity and hydrophilicity of the sulfonic acid groups in the 2,5-DABSA monomer structure, which played an important role in the membrane performance and properties. The presence of

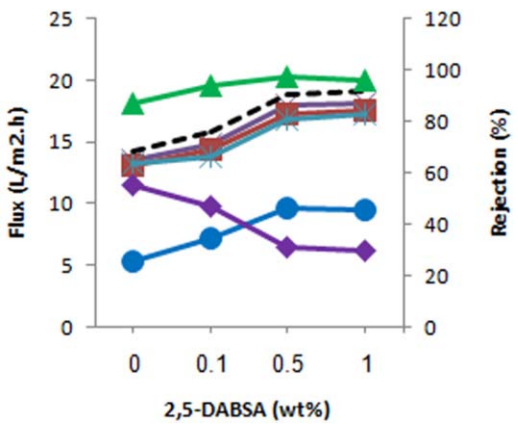

Figure 2. Effects of the 2,5-DABSA monomer concentration on the (- - -) pure water flux, NaCl (×) flux and (○) rejection, Na_2SO_4 (□) flux and (△) rejection, and $CaCl_2$ (*) flux and (◇) rejection. [Color figure can be viewed in the online issue, which is available at wileyonlinelibrary.com.]

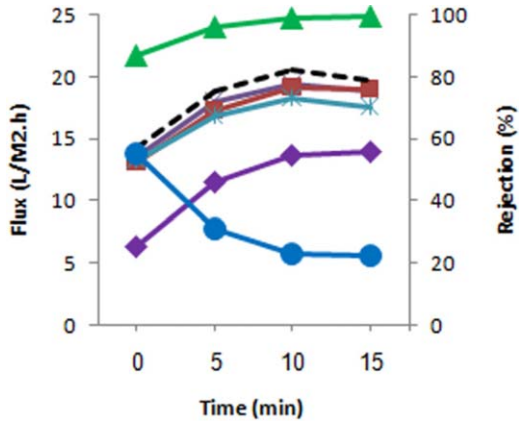

Figure 3. Effects of the modification time on the (—) pure water flux, NaCl (×) flux and (○) rejection, Na_2SO_4 (□) flux and (△) rejection, and $CaCl_2$ (*) flux and (◇) rejection. [Color figure can be viewed in the online issue, which is available at wileyonlinelibrary.com.]

sulfonic acids on the PA membrane surface resulted in the enhanced adsorption of water molecules onto the PA layer and an increase in the water permeate flux. However, with a further increase, the 2,5-DABSA monomer was not shown to change considerably with respect to the water permeate flux because no more acyl halide groups existed on the PA membrane surface for the reaction. The nascent PA layer had two chemical structures: (1) a crosslinked PA polymer, which consisted of three amide bonds with PIP, and (2) a linear PA polymer, which contained two amide bonds and a free pendant acyl chloride.[36] Free acyl chloride groups allowed the second modification of the PA membrane surface only with reactive chemical compounds because the high reactive acyl halide groups present when it was exposed caused the water molecules to be hydrolyzed to carboxylic acid groups. According to the relatively slow process of the hydrolysis reaction, the nascent PA layer was immediately modified with the reactive 2,5-DABSA monomers.[37]

The NaCl, Na_2SO_4, and $CaCl_2$ permeate fluxes and salt rejections are shown in Figure 2. The influence of the 2,5-DABSA monomer concentration was observed at 0.5%, and the greater concentration effects on the water permeate flux and salt

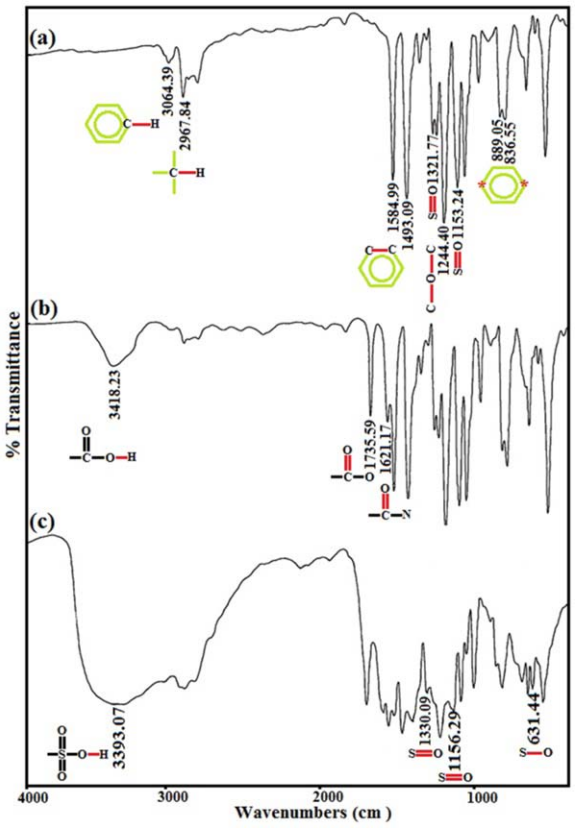

Figure 4. FTIR spectra of the (a) PSf substrate, (b) PA membrane, and (c) modified PA membrane. [Color figure can be viewed in the online issue, which is available at wileyonlinelibrary.com.]

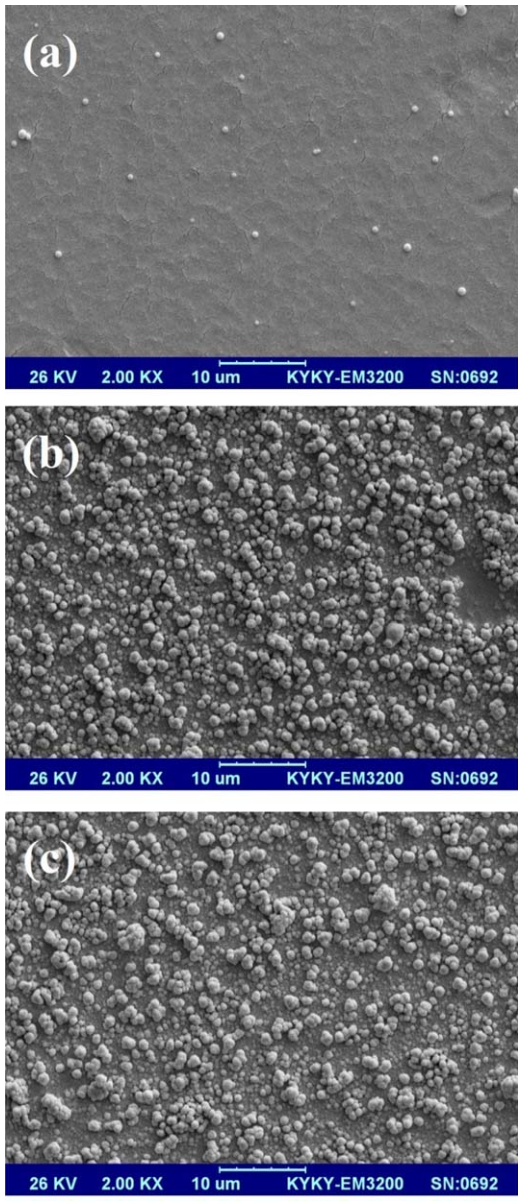

Figure 5. Surface SEM images of the (a) PSf substrate, (b) PA membrane, and (c) modified PA membrane. [Color figure can be viewed in the online issue, which is available at wileyonlinelibrary.com.]

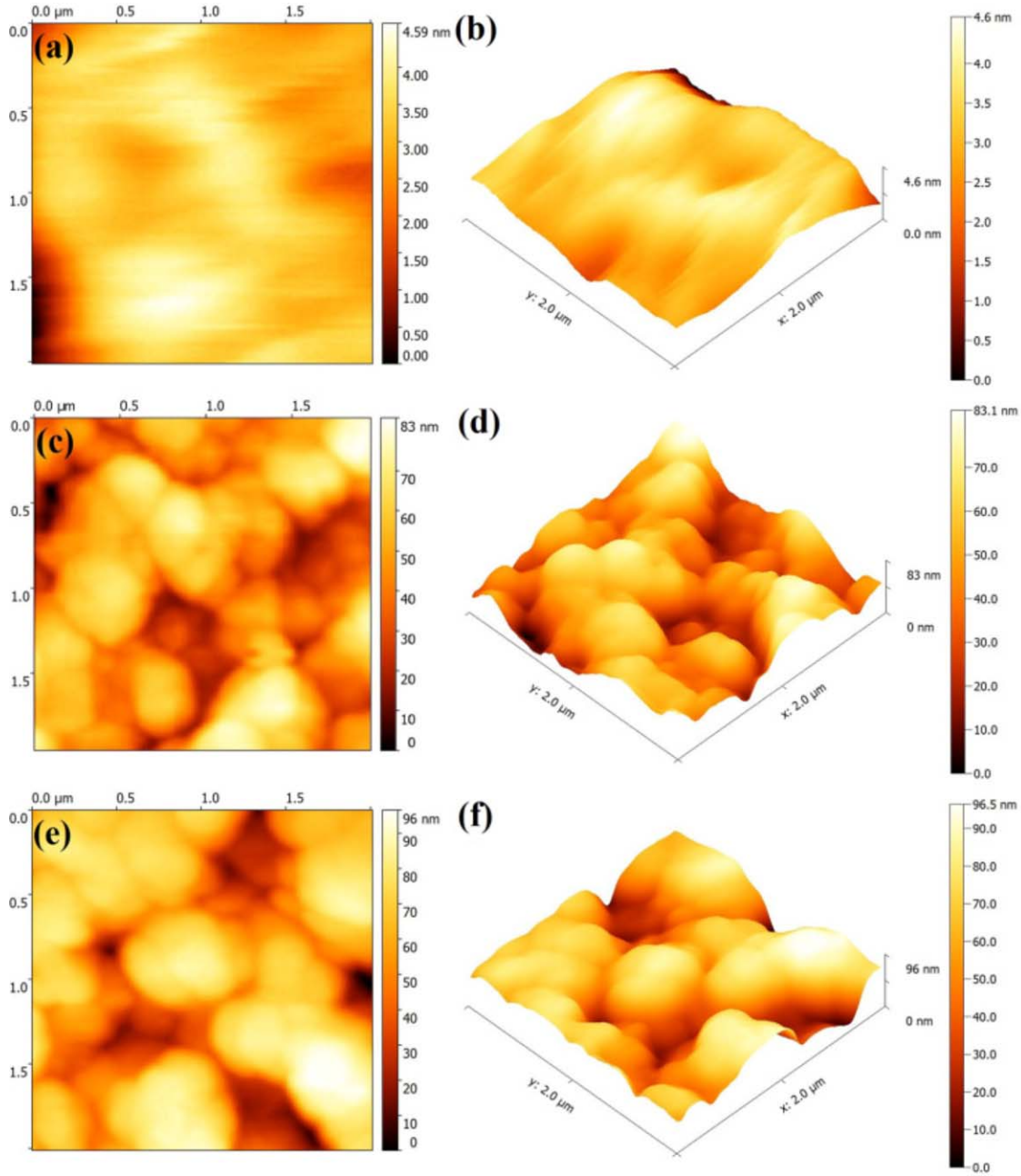

Figure 6. Surface AFM images of the (a,b) PSf substrate, (c,d) PA membrane, and (e,f) modified PA membrane. [Color figure can be viewed in the online issue, which is available at wileyonlinelibrary.com.]

rejections were not significant. With increasing water permeate flux, the NaCl and Na_2SO_4 salt rejections increased considerably. NaCl and Na_2SO_4 rejections of 25.5 and 87.1% in the PA membrane increased to 46.1 and 97.5% at a 0.5% 2,5-DABSA monomer concentration. However, the $CaCl_2$ salt rejection decreased from 55.2 to 31.2%; this indicated changes in the membrane surface charge.[38] The presence of sulfonic acid groups on the membrane surface led to the induction of negative charge effects. As a result, the order of salt rejection changes from $RNa_2SO_4 > RCaCl_2 > RNaCl$ for the PA membrane to $RNa_2SO_4 > RNaCl > RCaCl_2$ for the modified PA membrane.[39,40] The new salt rejection order indicated that the charges on the membrane surface after modification were changed to a negative charge because the anionic salt (Na_2SO_4) rejection increased,

Table I. Surface Roughness Parameters of the PSf Substrate, PA Membrane, and Modified PA Membrane

	S_a (nm)	S_q (nm)	S_z (nm)
PSF substrate	0.47	0.65	4.58
PA membrane	12.85	15.42	83.08
Modified PA membrane	13.46	16.74	96.45

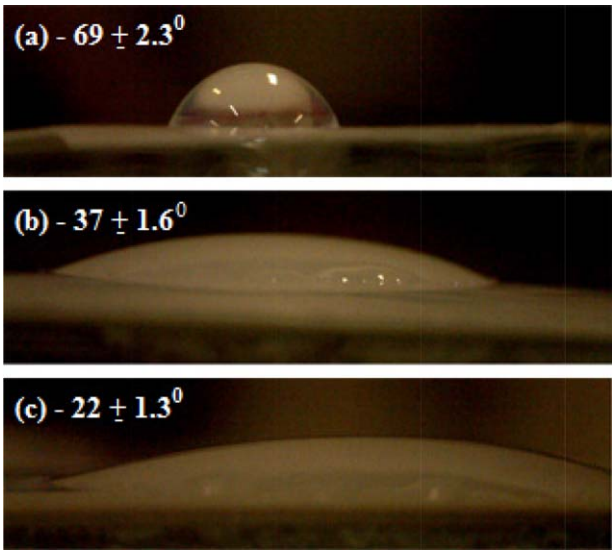

Figure 7. Contact angle images of the (a) PSf substrate, (b) PA membrane, and (c) modified PA membrane. [Color figure can be viewed in the online issue, which is available at wileyonlinelibrary.com.]

whereas the cationic salt ($CaCl_2$) rejection decreased. The second modification of the PA membrane with a 2,5-DABSA monomer containing sulfonic acid groups led to higher water permeability and monovalent and divalent anionic salt rejections.

Optimization of the Reaction Time

At a 0.5% w/w 2,5-DABSA monomer concentration, the modification time of the PA membranes was varied to 5, 10, and 15 min until optimized conditions were achieved for the second modification. The water permeate fluxes and salt rejections of NaCl, Na_2SO_4, and $CaCl_2$ are illustrated in Figure 3. As shown in Figure 3, with increasing modification time to 10 min, the water permeate flux reached 20.6 L m^{-2} h^{-1}; this indicated an increase of more than 44% in the pure water flux. At a 0.5% w/w concentration and with a 10-min modification time, the maximum number of acyl chloride groups reacted with the 2,5-

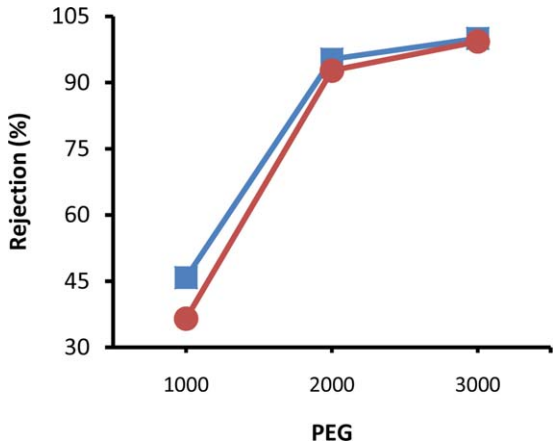

Figure 8. Rejection of PEGs of different molecular weights with the (□) PA and (○) modified PA membranes. [Color figure can be viewed in the online issue, which is available at wileyonlinelibrary.com.]

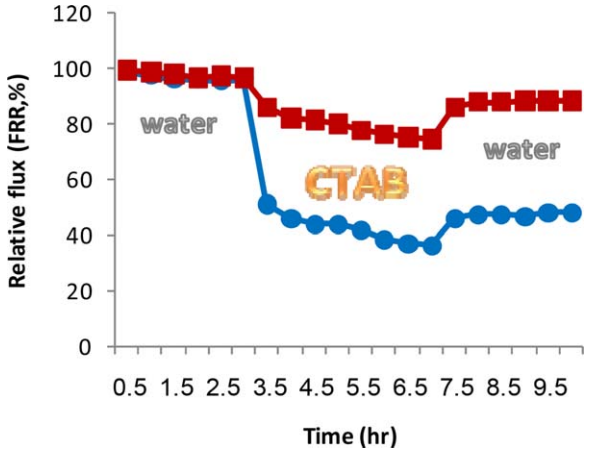

Figure 9. Fouling experiments: (○) PA and (□) modified PA membranes. [Color figure can be viewed in the online issue, which is available at wileyonlinelibrary.com.]

DABSA monomer or were hydrolyzed by water and neutralized. At the same 2,5-DABSA monomer concentration, rejections of NaCl and Na_2SO_4 salt increased and reached 54.7 and 99.2%, respectively. Similarly, $CaCl_2$ salt rejection decreased to a minimum value of 22.9%; this indicated that the PA membrane modification reached to the highest possible level. Because at the further modification time (15 min) no significant changes were observed in the water permeate flux and salt rejection, the 10-min modification time was considered to be the optimized time.

Investigation of the Chemical Composition of the Membranes

The FTIR spectra of the PSf substrate, PA membrane, and modified PA membrane are shown Figure 4. The PSf substrate spectra displayed peaks of the stretching vibrations of C—H aliphatic and aromatic bonds at 2967 and 3084 cm^{-1}.[41] Two strong peaks at 1493 and 1584 cm^{-1} were related to the C=C bonds in the straining vibrations of the benzene rings. The symmetric and asymmetric stretching vibrations of S=O bonds were observed at 1153 and 1321 cm^{-1}, respectively. Also, the sharp peak at 1244 cm^{-1} corresponded to ether bonding (C—O—C) of the PSf structure. Two peaks at 836 and 869 cm^{-1} were assigned to the para situation of benzene rings in the PSf chemical structure.

Figure 4(b) illustrates FTIR analysis of the PA nanofiltration membrane; this consisted of three new peaks at 1621, 1735, and 3418 cm^{-1}; these were attributed to the C=O stretching vibrations of carboxylic acid and amide groups and O—H bonds of carboxylic acid groups, respectively.[42] The FTIR spectra of the PA membrane confirmed that interfacial polymerization was successfully carried out on the surface of the PSf substrate.

The modified PA membrane spectrum is shown in Figure 4(c); it showed new peaks attributed to the 2,5-DABSA monomer. Two peaks at 1156 and 1330 cm^{-1} were assigned to S=O symmetric and asymmetric stretching vibration bonds in the 2,5-DABSA monomer and PSf structures that shifted to higher wavelengths.[43] The stretching vibrations of the S—O bond of the sulfonic acid group were observed seen at 631 cm^{-1}, and

Table II. Performance of the PA and Modified PA Membranes in the Presence of a CTAB Solution

Membrane	J_{w1} (L m^{-2} h^{-1})	J_p (L m^{-2} h^{-1})	J_{w2} (L m^{-2} h^{-1})	FRR (%)	R_{ir} (%)	R_r (%)	R_t
PA membrane	13.8	6.6	6.6	47.8	52.1	10.1	62.2
Modified PA membrane	21.1	16.3	18.8	89	11.8	10.9	22.7

the hydroxyl groups of sulfonic acid showed a broad peak at 3393 cm^{-1}. These peaks proved that the 2,5-DABSA monomers modified the PA nanofiltration membrane surface.

Membrane Surface Morphology

SEM. Figure 5 shows SEM images of the PSf substrate, PA nanofiltration membrane, and modified PA membrane at 2000× magnification. The PSf substrate image illustrates the smoothness and integrity of the surface; this proved that the casting of the polymer solution and phase-inversion process were properly done. However, in Figure 5(b), a completely different morphology is shown; this confirmed that the interfacial polymerization reaction occurred on the PSf substrate, and the PA layer formed uniformly. Over the SEM image, there was a nodular structure with different sizes of nodules. Also, the modified PA membrane [Figure 5(c)] illustrated that the same dispersion and morphology covered the surface entirely. The 2,5-DABSA monomers had a molecular size, and free acyl chloride partially was dispersed over the PA membrane surface. As a result, the PA membrane surface morphology was unchanged after the second modification.

AFM. The two- and three-dimensional AFM images obtained for the PSf substrate, PA membrane, and modified PA membrane are presented in Figure 6. Also, different parameters, such as S_a, S_q, and S_z, of the samples were quantified from the AFM data, as presented in Table I. As shown in Figure 6, the surface morphology of the PA membrane was quite different from that of the PSf substrate, and it showed a homogeneous finely structure over the surface. Also, the roughness parameters, S_a, S_q, and S_z, of the PA membrane increased from 0.47, 0.65, and 4.58 nm to 12.85, 15.42, and 83.08 nm, respectively. The higher roughness parameters of the PA membrane were due to the formed three-dimensional crosslinked PA polymer with regard to the spatial arrangement of the TMC monomer. As shown in Figure 6(e,f), the second modification of the PA membrane with the 2,5-DABSA monomer did not lead to significant changes in the surface morphology, and a fine structure evenly covered the modified PA surface. Also, the modified PA surface roughness increased only 0.61 nm, which was negligible. The results prove that the study of sulfonic acid on the PA layer with this method did not lead to a swollen PA active skin layer.

Hydrophilicity of the Membranes

The dry membranes used to determine the contact angle by the sessile drop technique are illustrated in Figure 7. A lower contact angle indicated a higher hydrophilicity because a greater tendency for water molecules to wet the membrane surface existed. The PSf substrate exhibited a contact angle of 69 ± 2.3°; this indicated initial resistance against the water molecules and relatively hydrophobic properties. After interfacial polymerization, the PA membrane hydrophilicity was improved, and it decreased to 37 ± 1.6°; this indicated that the PA layer was moderately hydrophilic. Functional groups, such as such as amide, amine, carboxylic acid, and sulfonic acid groups, in the PA membrane structure had major effects on the hydrophilicity. However, with the second modification of the PA membranes with the 2,5-DABSA monomer, the contact angle reached 22 ± 1.3°. The lower contact angle of the modified PA membrane indicated very hydrophilic properties and existed because of the presence of polar and hydrophilic groups of sulfonic acids in the 2,5-DABSA monomer structure. The results of the PA and modified membranes showed good agreement with the permeability data and confirmed that a higher hydrophilicity was achieved with modification by the 0.5% w/w 2,5-DABSA monomer.

MWCO

Three low-molecular-weight PEGs (1000, 2000, and 3000 Da) were used in MWCO determination by Causserand's protocol. Figure 8 shows the rejections of the prepared PA and modified PA membranes to different molecular weight PEGs. As shown in Figure 8, rejection increased with the growth of the PEG molecular weight from 1000 to 3000 Da. From the rejection behavior (corresponding to a rejection of 90%), we found that the MWCOs of the PA and modified PA nanofiltration membranes were about 1909 and 1953 Da, respectively. Also, with eqs. (3) and (4), the average membrane pore sizes measured for PA and modified PA membranes were 1.81 ± 0.2 and 1.83 ± 0.2 nm. A slight change in the membrane pore size after the second modification proved interaction between the sulfonic acid groups and a swelling phenomenon. In this method, the PA layer formed in normal chemical processes with the high-molecular-weight PA polymer was established on the PSf substrate. The appropriate distribution of free acyl chloride over nascent PA enabled a second modification with minimum physicochemical property changes.

Fouling Experiments

CTAB with a hydrophobic chain and hydrophilic and cationic head was used as a contaminant in the fouling experiment with a negatively charged membrane surface by absorption or ionic interaction.[33] To investigate the influence of the 2,5-DABSA monomer on the fouling properties of the PA and modified PA membranes, we obtained the R_r, R_{ir}, R_t, and FRR values, as shown in Figure 9 and Table II. As shown, the FRRs of the PA and modified PA membranes decreased when CTAB (cationic surfactant, 1500 ppm) was used as the feed solution. As shown, the modified PA membrane showed relatively better antifouling properties because of the presence of sulfonic acid groups on the PA layer surface. Despite the higher negative charge of the modified PA membrane compared to the PA membrane and the

higher absorption of the CTAB contaminant on the membrane surface, R_t was lower. This phenomenon was probably due to the lower contact angle and higher hydrophilicity of the modified PA membrane, which conquered the membrane surface charge. The results in Table II reveal that FRR of the modified PA membrane increased 41.2%, whereas R_t of this membrane decreased 39.5%. Also, R_r of the modified PA membrane increased partially by 1.7% and R_{ir} decreased by 41.2% after the second modification; this indicated an important change in the membrane fouling properties.

CONCLUSIONS

In this research, we focused on the development of PA membrane permeability and antifouling properties with the grafting of 2,5-DABSA monomer with a simple and novel idea. The PA membrane was successfully modified with PIP and TMC monomers in an interfacial polymerization reaction. The free acyl chloride groups of the nascent PA layer were used for a second modification by the 2,5-DABSA monomer; this included two amines for the amidation reaction and one sulfonic acid group for the promotion of the PA membrane permeability, charge, and antifouling properties. The pure water flux of the modified PA membrane was enhanced as the 2,5-DABSA monomer content and modification time were increased, and it reached more than 44% for the PA membrane. The modification of the PA membrane led to a higher negative charge and a change in the salt rejection sequence from $RNa_2SO_4 > RCaCl_2 > RNaCl$ to $RNa_2SO_4 > RNaCl > RCaCl_2$. The SEM and AFM images indicated that the novel modification of the PA membrane morphology did not significantly change, and there was no sign of swelling. Also, the MWCOs of the PA and modified PA membranes were 1909 and 1953 Da; there was no significant difference. The study of the hydrophilicity indicated that the modified PA membrane, with a contact angle of 22°, has a great hydrophilicity, and this phenomenon led to a higher permeability flux. The modified PA membrane generally demonstrated an improved R_t to the CTAB cationic surfactant. R_t decreased from 52.5 to 22% because of the dispersion of sulfonic acid groups over the PA layer surface. As a result, this work offers the use of monomer-carrying sulfonic acid to increase positive effects (water permeate flux, hydrophilicity and antifouling properties) and to minimize of negative results (swelling, roughness, morphological conversion, and lower rejection). It is believed that the PA membranes modified by 2,5-DABSA monomer have great potential in the fabrication of PA nanofiltration membranes with high permeability and good antifouling properties.

REFERENCES

1. Weatherley, L. R. Engineering Processes for Bioseparation; Butterworth-Heinemann: New York, **1994**.
2. Wei, X.; Wang, Z.; Chena, J.; Wang, J.; Wang, S. *J. Membr. Sci.* **2010**, *346*, 152.
3. Cadotte, J. E.; Petersen, R. J.; Larson, R. E.; Erickson, E. E. *Desalination* **1980**, *32*, 25.
4. Wu, C.; Zhang, S.; Yang, D.; Jian, X. *J. Membr. Sci.* **2009**, *326*, 429.
5. Akbari, A.; Mojallali Rostami, S. M. *J. Water Reuse Desalination* **2014**, *4*, 174.
6. Lopes, C. N.; Carlos, J.; Petrus, C.; Riella, H G. *Desalination* **2005**, *172*, 77.
7. Chakrabarty, S.; Purkait, M. K.; Gupta, S. D.; De, S.; Basu, J. K. *Sep. Purif. Technol.* **2003**, *31*, 141.
8. Uyak, V.; Koyuncu, I.; Oktem, I.; Cakmakci, M.; Toroz, I. *J. Hazard. Mater.* **2008**, *152*, 789.
9. DerBruggen, B. V.; Everaert, K.; Wilms, D.; Vandecasteele, C. *J. Membr. Sci.* **2001**, *193*, 239.
10. Koyuncu, I.; Kural, E.; Topacik, D. *Water Sci. Technol.* **2001**, *43*, 233.
11. Jegal, J.; Min, S. G.; Lee, K. H. *J. Appl. Polym. Sci.* **2002**, *86*, 2781.
12. Rana, D.; Matsuura, T. *Chem. Rev.* **2010**, *110*, 2448.
13. Agenson, K. O.; Urase, Y. *Sep. Purif. Technol.* **2007**, *55*, 147.
14. Li, J. H.; Xu, Y. Y.; Zhu, L. P.; Wang, J. H.; Du, C. H. *J. Membr. Sci.* **2009**, *326*, 659.
15. Louie, J. S.; Pinnau, I.; Ciobanu, I.; Ishida, K. P.; Ng, A.; Reinhard, M. *J. Membr. Sci.* **2006**, *280*, 762.
16. Greenlee, L. F.; Lawler, D. F.; Freeman, B. D.; Marrot, B.; Moulinc, P. *Water Res.* **2009**, *43*, 2317.
17. Kang, G. D.; Cao, Y. M. *Water Res.* **2012**, *46*, 584.
18. Abu Seman, M. N.; Khayet, M.; Hilal, N. *Desalination* **2011**, *273*, 36.
19. Tarboush, B. J. A.; Rana, D.; Matsuura, T.; Arafat, H. A.; Narbaitz, R. M. *J. Membr. Sci.* **2008**, *325*, 166.
20. Zhang, Y.; Su, Y.; Chen, W.; Peng, J.; Dong, Y.; Jiang, Z.; Liu, H. *J. Membr. Sci.* **2011**, *382*, 300.
21. Zhou, C.; Ye, D.; Jia, H.; Yu, S.; Liu, M.; Gao, C. *Desalination* **2014**, *351*, 228.
22. Ni, L.; Meng, J.; Li, X.; Zhang, Y. *J. Membr. Sci.* **2014**, *451*, 205.
23. Zhou, Y.; Yu, S.; Liu, M.; Gao, C. *J. Membr. Sci.* **2006**, *270*, 162.
24. Liu, Y.; Zhang, S.; Zhou, Z.; Ren, J.; Geng, Z.; Luan, J.; Wang, G. *J. Membr. Sci.* **2012**, *394*, 218.
25. Xie, W.; Geisea, G. M.; Freeman, B. D.; Lee, H. S.; Byun, G.; McGrath, J. E. *J. Membr. Sci.* **2012**, *403*, 152.
26. Yong, Z.; Sanchuan, Y.; Meihong, L.; Congjie, G. *J. Membr. Sci.* **2006**, *270*, 162.
27. Afonso, M. D.; Hagmeyer, G.; Gimbel, R. *Sep. Purif. Technol.* **2001**, *22*, 529.
28. Chakrabarty, B.; Ghoshal, A. K.; Purkait, M. K. *J. Membr. Sci.* **2008**, *309*, 209.
29. Causserand, C.; Rouaix, S.; Akbari, A.; Aimar, P. *J. Membr. Sci.* **2004**, *238*, 177.
30. Sabde, A. D.; Trivedi, M. K.; Ramachandhran, V.; Hanra, M. S.; Misra, B. M. *Desalination* **1997**, *114*, 223.
31. Wang, Y. Q.; Su, Y. L.; Ma, X. L.; Sun, Q.; Jiang, Z. Y. *J. Membr. Sci.* **2006**, *283*, 440.

32. Peng, J.; Su, Y.; Shi, Q.; Chen, W.; Jiang, Z. *Bioresour. Technol.* **2011**, *102*, 2289.
33. Ghosh, A. K.; Hoek, E. M. V. *J. Membr. Sci.* **2009**, *336*, 140.
34. Schaep, J.; Vandecasteele, C. *J. Membr. Sci.* **2001**, *188*, 129.
35. Huang, R. H.; Chen, G. H.; Yang, B. C.; Gao, C. *J. Sep. Purif. Technol.* **2008**, *61*, 424.
36. Duan, M.; Wang, Z.; Xu, J.; Wang, J.; Wang, S. *Sep. Purif. Technol.* **2010**, *75*, 145.
37. Solomon, M. F. J.; Bhole, Y.; Livingston, A. G. *J. Membr. Sci.* **2012**, *423*, 371.
38. Kim, S. H.; Kwak, S. Y.; Susuki, T. *Environ. Sci. Technol.* **2005**, *39*, 1764.
39. Kang, G.; Liu, M.; Lin, B.; Cao, Y.; Yuan, Q. *Polymer* **2007**, *48*, 1165.
40. Peeters, J. M. M.; Boom, J. P.; Mulder, M. H. V. *J. Membr. Sci.* **1998**, *145*, 199.
41. Singh, P. S.; Joshi, S. V.; Trivedi, J. J.; Devmurari, C. V.; Rao, A. P.; Ghosh, P. K. *J. Membr. Sci.* **2006**, *278*, 19.
42. Saha, N. K.; Joshi, S. V. *J. Membr. Sci.* **2009**, *342*, 60.
43. Chen, G.; Li, S.; Zhang, X.; Zhang, S. *J. Membr. Sci.* **2008**, *310*, 102.